Ionospheric redistribution during geomagnetic storms

T. J. Immel[1] and A. J. Mannucci[2]

Received 3 April 2013; revised 29 October 2013; accepted 1 November 2013; published 27 December 2013.

[1] The abundance of plasma in the daytime ionosphere is often seen to grow greatly during geomagnetic storms. Recent reports suggest that the magnitude of the plasma density enhancement depends on the UT of storm onset. This possibility is investigated over a 7 year period using global maps of ionospheric total electron content (TEC) produced at the Jet Propulsion Laboratory. The analysis confirms that the American sector exhibits, on average, larger storm time enhancement in ionospheric plasma content, up to 50% in the afternoon middle-latitude region and 30% in the vicinity of the high-latitude auroral cusp, with largest effect in the Southern Hemisphere. We investigate whether this effect is related to the magnitude of the causative magnetic storms. Using the same advanced *Dst* index employed to sort the TEC maps into quiet and active (*Dst* < –100 nT) sets, we find variation in storm strength that corresponds closely to the TEC variation but follows it by 3–6 h. For this and other reasons detailed in this report, we conclude that the UT-dependent peak in storm time TEC is likely not related to the magnitude of external storm time forcing but more likely attributable to phenomena such as the low magnetic field in the South American region. The large *Dst* variation suggests a possible system-level effect of the observed variation in ionospheric storm response on the measured strength of the terrestrial ring current, possibly connected through UT-dependent modulation of ion outflow.

Citation: Immel, T. J., and A. J. Mannucci (2013), Ionospheric redistribution during geomagnetic storms, *J. Geophys. Res. Space Physics*, *118*, 7928–7939, doi:10.1002/2013JA018919.

1. Introduction

[2] Over the past 15 years, significant new details of the global-scale morphology of the positive ionospheric storm have been revealed by new imaging techniques. The positive storm is a regional-scale condition of the ionosphere occurring during geomagnetic disturbances during which plasma densities are driven above values normally observed during quiescent periods [*Buonsanto*, 1999]. New imaging techniques have provided regional and global-scale maps of the storm time variation of ionospheric density, using radio occultation, ultraviolet imaging, and active radar approaches, described later in this report. The key point is the new recognition that the morphology of storm-enhanced density exhibits remarkable structure with sharp boundaries, with concomitant effects in the ionosphere and plasmasphere [*Foster et al.*, 2002; *Goldstein*, 2006]. A new view of the geospace system has thus emerged that opens additional questions about the coupling and interaction of ionospheric and magnetospheric plasma. In particular, one must consider the roles of feedback processes and system preconditioning when evaluating the behavior of coupled systems.

[3] This report seeks to describe the fundamental change in the ionosphere during periods of high geomagnetic activity. As will be shown, the predominant effect is the daytime enhancement in ionospheric plasma density, deduced from measurements of enhanced electron content derived from radio occultations. This growth in ionospheric plasma densities during geomagnetic storm periods has been previously investigated at length [cf. *Mendillo et al.*, 1970, 1972; *Buonsanto*, 1995], with a number of competing effects identified as playing some role in driving these changes including large-scale gravity waves [*Immel et al.*, 2001; *Prölss*, 2008], magnetospheric convection electric fields [*Lanzerotti et al.*, 1975; *Foster*, 1993], and storm time wind disturbances [*Jones and Rishbeth*, 1971; *Anderson*, 1976]. Each of these effects clearly can affect the ionosphere individually. It is usually a question of which are operative in particular geographic regions/local times, combining or interacting with another driver, and during which phase of a particular disturbance they occur or dominate.

[4] The main *F* layer is not the only region where enhanced ionospheric plasma densities are observed during geomagnetic events. The flow of terrestrial ionospheric O^+ from the polar regions into the surrounding magnetosphere during geomagnetic storms contributes to enhanced plasma pressure and pressure gradients in the inner magnetosphere during the hours that follow storm onset. This effect has

[1]Space Sciences Laboratory, University of California, Berkeley, California, USA.
[2]Jet Propulsion Laboratory, Pasadena, California, USA.

Corresponding author: T. J. Immel, Space Sciences Laboratory, University of California, Berkeley, CA 94720, USA. (immel@ssl.berkeley.edu)

2169-9380/13/10.1002/2013JA018919

been discerned by numerous spaceborne experiments [cf. *Sharp et al.*, 1976; *Daglis et al.*, 1993; *Lui et al.*, 2005], and the processes are captured in sophisticated numerical models of the ring current [*Fok et al.*, 1993; *Liemohn et al.*, 1999] and of the overall solar wind-magnetosphere-ionosphere coupling [cf. *Zhang et al.*, 2007]. Combined with enhanced density and earthward convection of magnetospheric plasma originating in the solar wind, an increase in the westward oriented magnetospheric "ring current" encircling the earth is observed during storms. This current results in a reduction of the northward oriented terrestrial magnetic field measured at low and middle latitudes [*Clauer and McPherron*, 1974; *Akasofu*, 1981]. Though the oxygen ions are lost rapidly (relative to the normally greater proton population) through charge exchange reactions with the hydrogen exosphere, they are estimated to constitute 50% or more of the total magnetospheric ring current at the peak in its intensity during the main phase of strong geomagnetic storms [*Daglis*, 1997; *Liemohn et al.*, 1999].

[5] It is in this context that we research the development of ionospheric enhancements during magnetic storms. For the fact that ionospheric plasma is a key constituent of the magnetospheric plasma during storms, it is possible that the enhancement of ionospheric plasma densities, the various processes that produce that effect, and the resultant longitudinal and local time dependencies in plasma production and transport may affect how the magnetosphere is loaded with ionospheric plasma.

[6] An important, limiting condition on the flux of outflowing plasma is the abundance of ionospheric O^+ in the high-latitude outflow region. Some key processes exert control over said abundance and are briefly noted here. Locally, ionization by solar EUV radiation is the primary source, with chemical recombination acting as the primary sink, mainly by interaction with N_2 [*Hunsucker and Hargreaves*, 2002]. As auroral precipitation sources increase, a region of progressively higher thermospheric [N_2/O] column concentration ratio develops in response to upwelling of molecular species driven by auroral and Joule heating of the neutral gas [*Prölss*, 1980; *Prölss and Roemer*, 1987; *Nicholas et al.*, 1997]. Secondary sources such as low-energy auroral precipitation and recombination losses such as that due to increased plasma convection are more variable. Due to the constant circulation of the thermospheric gas during storms, a slowly growing region with higher chemical loss rates develops in response to hours of accumulated heating around the auroral zone [*Roble*, 1977; *Fuller-Rowell et al.*, 1996]. This region impinges upon the daytime ionosphere with a delay of 3–6 h [*Immel et al.*, 2001]. Therefore, early in a geomagnetic storm, the daytime O^+ abundance can be readily enhanced by advection of O^+-rich plasma into the daytime cusp region from lower latitudes, avoiding passage through regions of high chemical loss rates. As the magnetospheric convection expands to lower latitudes where ion production driven by solar EUV is greatest and the tilt of the magnetic field toward the equator increases, plasma is generally convected poleward and to higher altitudes ($\mathbf{v_i} = (\mathbf{E} \times \mathbf{B})/B^2$). This has the effect of reducing recombination and providing an additional enhancement over what would be expected to arrive in the vicinity of the cusp through only direct (horizontal) transport [*Foster*, 1993; *Heelis et al.*, 2009].

[7] The new capability for measuring the global-scale redistribution of ionospheric plasma during storms, made possible by satellite constellations like the Global Positioning System (GPS) combined with extensive ground networks of dual-band GPS receivers [*Mannucci et al.*, 1998; *Kintner et al.*, 2003] as well as ultraviolet imaging of ionospheric plasma from space, reveals global- and regional-scale ionospheric structures that emerge during geomagnetic storms [*Foster et al.*, 2005; *Immel et al.*, 2005]. The ionosphere develops large regions of storm-enhanced density (SED) on the dayside, extending from middle latitudes after noon to high latitudes near noon, the latter being the general vicinity of field lines that extend out to the magnetospheric cusp. Plasma rapidly streams along the poleward boundary of these regions at speeds of 1 km s^{-1} and higher [*Foster*, 1989; *Pryse et al.*, 2004], driven by electric fields in flow channels known as subauroral polarization streams (SAPS) [*Goldstein et al.*, 2003]. The SAPS phenomenon, and associated rapid transport of O^+ from middle to high latitudes, clearly has the potential to affect the abundance of plasma in the high-latitude outflow region. As such, it is a key process that has only recently been considered in the global context of the system-level effects of ionospheric outflow during storms.

[8] Numerical simulations by *Zeng and Horwitz* [2008] demonstrate the importance of these storm time transport effects in enhancing high-latitude ion outflow from the daytime cusp. Their work showed that the enhancement of *F* region densities in the cusp by a SAPS-driven plume could contribute to ion outflow in a manner similar to the precipitation of soft electrons, another key factor in the regulation of outflow [*Strangeway et al.*, 2000]. Furthermore, if these storm time plasma transport effects vary with longitudinal sector as recent observations suggest [*Foster et al.*, 2005; *Coster et al.*, 2007], a corresponding UT variation in outflow flux, inner magnetospheric plasma pressure, and, ultimately, geomagnetic storm strength may exist. Thus, it is important to undertake a systematic investigation of the redistribution of plasma during geomagnetic storms. Here this is performed using 7+ years of data-driven, global-scale assimilative maps of ionospheric density. If there is a dependence of the density of storm-enhanced density effects on UT, then a signature of that effect may be evident in this database.

2. GPS Total Electron Content Maps

[9] To obtain a consistent global measure of ionospheric conditions, we make use of global maps of ionospheric total electron content (TEC). These are created from GPS-determined TEC and provide 2.5° × 5.0° latitude-longitude resolution in 2 h time steps. The maps are openly available, determined at Jet Propulsion Laboratory (JPL) using the method described by *Mannucci et al.* [1998], using approximately 98 ground stations from 1999 to 2005 and nearly 200 stations in subsequent times up to the present day. The 2 h averaging and large spatial bins effectively smooth sharp gradients but are sufficient to determine the average global-scale storm and quiet-time ionospheric behavior. Data from 7 full years (1999–2005) and the latter half of 1998 are used, ordering the data into two major bins of low and high activity, defined in the next section. This period captures most of the large geomagnetic storms of the years 2000–2002 solar

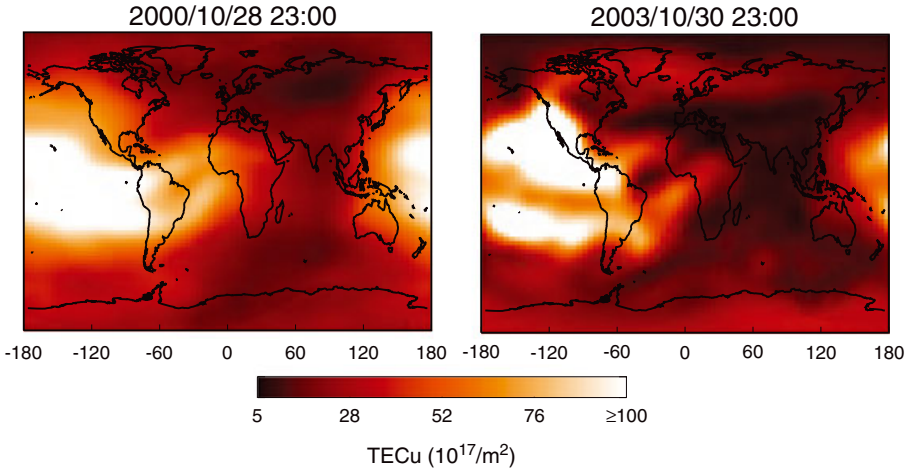

Figure 1. Two views of JPL-TEC maps, from a low magnetic activity period in 2000 and a high magnetic activity in 2003, from the same season and high levels of solar radio flux (daily 10.7 cm radio fluxes of 183.1 and 264.0 Jy, respectively).

maximum. To evaluate changes in the ionosphere produced by storms, the ratio of high to low activity TEC can then be compared at any geographic/magnetic location and/or local time.

[10] Two example maps showing inputs to the quiet and storm bins of data are shown in Figure 1. For this study, the level of the geomagnetic storm index, *Dst*, provides the sole criterion for determination of quiet and active times. On 28 October 2000, the mean *Dst* index for the 24 h preceding the collection of TEC data was approximately 0 nT. In contrast, the degree of activity on 30 October 2003 was extremely high, with the mean *Dst* preceding the time of the map reaching approximately –235 nT. The daily solar 10.7 cm radio flux is also higher in the latter case (264 Jy (jansky; 10^{-26} W m^{-2} Hz^{-1}) in 2003 versus 183 Jy in 2000), though the monthly mean solar flux in October is similar (155 and 167 Jy for 2003 and 2000, respectively). These times are selected to demonstrate representative changes in ionospheric plasma distribution produced by geomagnetic storm inputs under similar seasonal conditions. Simple visual inspection reveals major differences that are evident at all latitudes. One outstanding storm effect is the major storm time TEC enhancement at middle latitudes in daytime (noon is at –165 longitude). Large density enhancements over the northeastern Pacific and west coast of North America are evident, with steepened gradients in TEC around this feature. At lower latitudes, a significant reduction in TEC at the equator is evident, and at higher latitudes a trail of enhanced plasma density describes a path of plasma transport from dayside to night. This particular signature is due to the rapid advection of daytime plasma across the polar cap by enhancement in storm time magnetospheric convection and polarization electric fields [*Basu and Valladares*, 1999; *Foster et al.*, 2005].

[11] Away from the still highly accentuated equatorial bands and polar cross-cap plasma signature, nighttime plasma densities are lower in the storm time image. Though this presentation lacks additional information necessary to draw particular conclusions, reduced nighttime TEC may likely be attributed to storm effects including enhanced O^+ recombination rates due to both enhanced high-latitude convection [*Rodger et al.*, 1992; *Zou et al.*, 2011] and transport of molecular-rich parcels of heated thermospheric gas out of the polar cap and into the nighttime middle-latitude ionosphere [*Prölss and Roemer*, 1987].

3. Sorting JPL-TEC by UT and Dst_{LG}

[12] The year 2000 image on the left of Figure 1 shows data that were added to the "quiet" data set, and the year 2003 image on the right shows data that were added to the "active" set. These are selected for the mean value of *Dst* occurring during the 2 h window, the hourly index of geomagnetic activity. This index has been determined since the International Geophysical Year (1958) using measurements from four middle-latitude magnetometers separated from one another by roughly 90° of longitude [*Sugiura*, 1964]. In the determination of *Dst*, diurnal changes in overhead ionospheric electric currents are determined and subtracted in order to improve the use of *Dst* as a measure of inner magnetospheric currents. To date, the most exhaustive treatment and removal of diurnal ionospheric currents has been performed by *Love and Gannon* [2009], producing what is termed the $D_{st}^{5807-4SH}$ index. Its sophisticated quiet-time (Sq) current subtraction obviates several problems with the original method by which *Dst* is determined, in particular a UT-dependent effect identified recently by *Mursula et al.* [2010]. We select $D_{st}^{5807-4SH}$ for this statistical analysis of geomagnetic storms and refer to it hereafter simply as Dst_{LG}.

[13] Two sets of mean TEC maps are determined from the 7+ year TEC data set: "quiet" for $Dst_{LG} > -50$ nT and "active" for $Dst_{LG} < -100$ nT. These are determined for the 12 two-hour steps of UT in both activity ranges. The number of samples (complete maps) loaded in each set is saved, as well as the total of all mapped TEC values squared, to evaluate the statistical distribution of TEC values.

3.1. Geographic Maps of Mean JPL-TEC: Active Versus Quiet

[14] The mean TEC observed in each of the bins is shown in Figure 2. With 12 TEC maps a day for over 7 years,

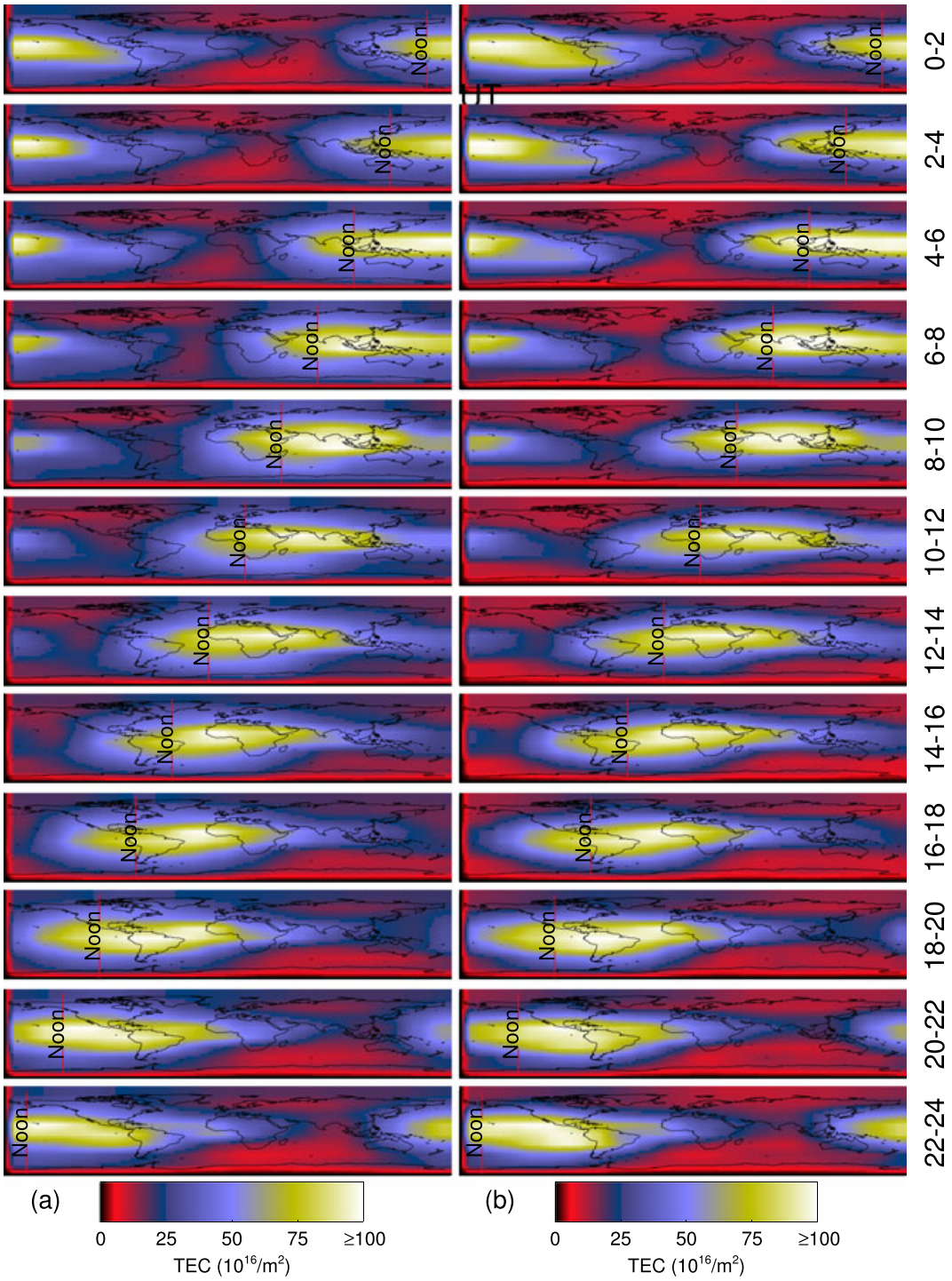

Figure 2. The mean TEC versus UT in the (a) quiet and (b) active Dst_{LG} bins.

there are roughly 45,000 sample maps, ∼90% of which are grouped in the quiet bin (Figure 2a) and ∼2% in the active bin (Figure 2b). The data in the intervening *Dst* range are not shown. In each map the continents are shown and "Noon" is indicated with a vertical line, with UT of the 2 h maps increasing from top to bottom on the page. Even with the major difference in sample size and geomagnetic conditions, the overall features of quiet and storm times do not appear exceedingly different, exhibiting the same progression of high TEC near the equator toward the west and extended bands of high TEC about the magnetic equator into nighttime. To reveal the major changes that do occur under storm conditions, differences between the active and quiet cases in each UT bin are determined and shown in Figure 3.

[15] The TEC differences in each UT range (active TEC-quiet TEC) are shown in Figure 3a. A mean storm time enhancement of 10–30 TECU (total electron content units; 1 TECU = 10^{16} el m^{-2}) is observed over most low-latitude

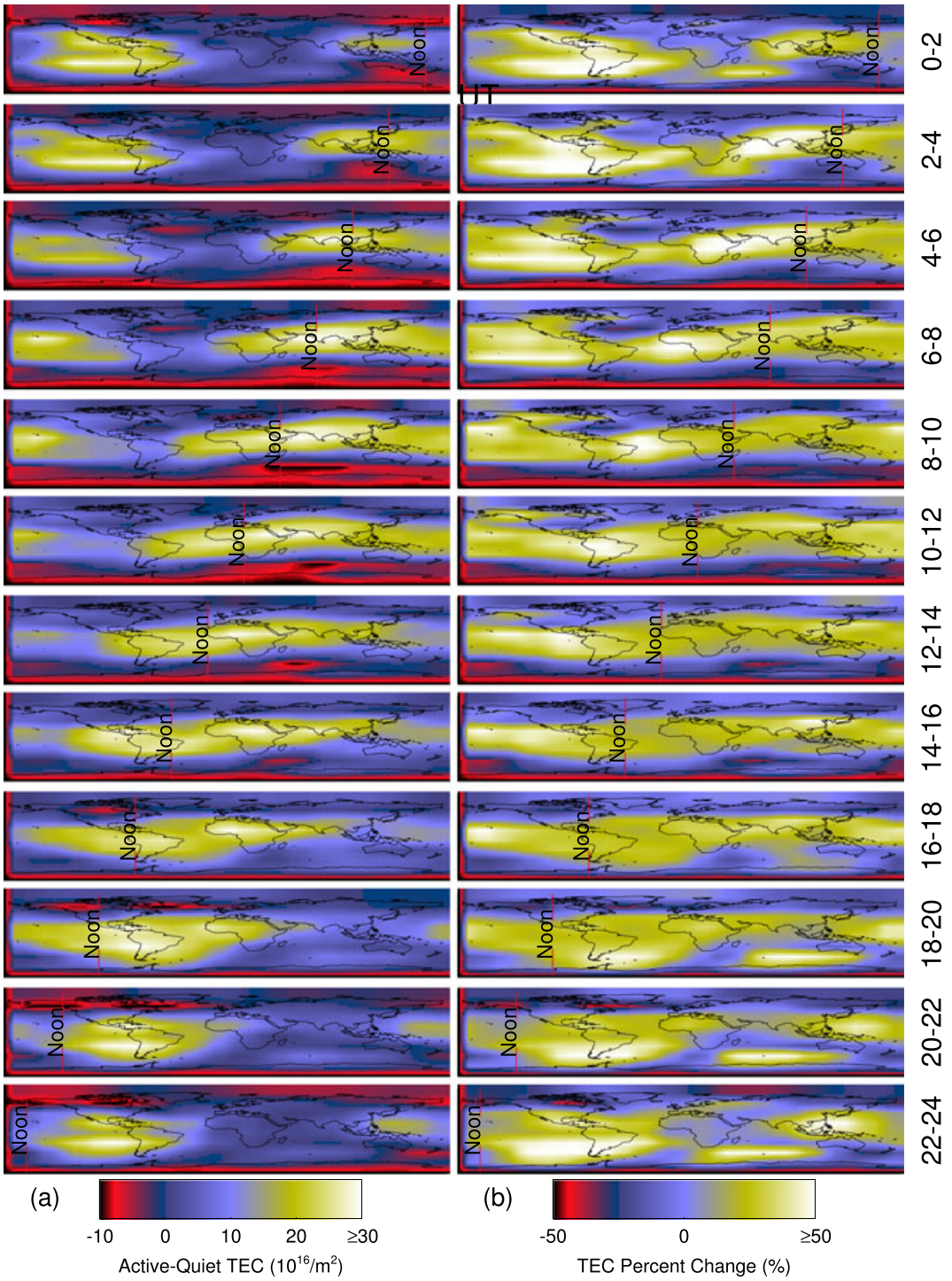

Figure 3. (a) The difference between the mean TEC in active and quiet Dst_{LG} bins. (b) The percent difference of the storm TEC values from the quiet TEC values.

locations, with some TEC reductions at middle and high latitudes. The enhancement is generally greatest in daytime, extending across the noon sector with a postnoon peak. Interestingly, as the noon line crosses the Pacific beginning around 20 UT, the region of heightened TEC remains in the afternoon sector (east of the noon line) over the Americas. This region continues to exhibit a storm time enhancement higher than that observed in the noon sector until 4 UT. This is remarkable for the fact that by this time the Eastern Pacific has been in the dark for several hours. Thus, the enhancement is likely a signature of earlier storm time production in sunlit conditions. This tendency for TEC to grow rapidly in a geographic sector and then corotate was described by *Foster et al.* [2005] as a plasmaspheric bulge. It is also in this sector where the most significant two-banded structure appears in the afternoon,

another indication of greater uplift and plasma production in daytime in the American sector as compared to others. Some possible explanations of this longitudinal variation are discussed in the following sections of this report.

[16] The global-scale changes in TEC are also generally consistent with expected changes in thermospheric composition. These changes are driven by auroral and Joule heating [*Prölss and Craven*, 1998; *Immel et al.*, 2000; *Strickland et al.*, 2001], primarily resulting in greatly enhanced molecular mixing ratios throughout the column of thermospheric gas at high latitudes. This high-latitude composition disturbance effect expands to lower latitude through meridional transport by enhanced thermospheric winds [cf. *Fuller-Rowell et al.*, 1991] with the effect of reducing ionospheric densities through chemical recombination. On the other hand, at middle to low latitudes the convergence of storm time winds can enhance downward transport, with the result of enhancing the relative abundance of light atmospheric constituents including atomic oxygen. Previous reports of this effect have found it to be particularly effective in the afternoon and later local times [*Burns et al.*, 1995; *Immel et al.*, 2001]. On the overall time scale of a magnetic storm (12–36 h), this composition effect combines with other wind and electric field effects to enhance low-latitude O^+ production during storms.

[17] In the storm time TEC averages presented here, composition effects are at least partly responsible for the middle-latitude reduction in TEC that is most evident around the times when the auroral oval and respective magnetic pole are tilted toward the dayside (4–10 UT in the Southern Hemisphere and 16–24 UT in the Northern Hemisphere) [*Nicholas et al.*, 1997; *Prölss and Craven*, 1998]. Near the equator, the overall enhancement of TEC could be supported in part by redistribution of thermospheric constituents and downward transport of atomic oxygen near the equator. However, composition variation has never been shown to vary in a manner that would account for the change in the structure of the TEC enhancement with UT or the general preference for larger enhancement in the American sector.

[18] Examining the TEC differences as percent changes from quiet levels (Figure 3b) gives additional insight into the storm time variations. First, one can again see that the South American sector suffers the largest TEC enhancement during storms, from 18 UT to 4 UT (from 14 to 24 LT in Central South America) . Another storm effect can be seen: the morning sector (west of the noon line) shows a very consistent increase over quiet-time values at every UT. Because the morning sector densities are relatively low, viewing differences in percent of TEC reveals this interesting effect. Unlike the postnoon enhancement, the local time of the greatest morning enhancement is regularly 4–6 h from noon, close to the morning terminator. One possible explanation for this enhancement is the favorable thermospheric composition that develops during storms (discussed above) where production of O^+ may immediately exceed quiet-time levels with the arrival of daylight. Further investigation of this secondary effect is an appropriate topic for a separate research effort and is outside the scope of this report.

[19] In summary, storm time TEC enhancements are observed broadly in latitude and longitude, with most significant enhancement and structuring observed after 18 UT in the afternoon sector. This UT/LT combination corresponds to the American longitudinal sector, and only in this sector does the enhancement persist well after sunset. The Asian sector also shows a strong storm time enhancement, but it is situated over the magnetic equator, while the American enhancement grows on either side of the equator, with much larger area of relative (percent) enhancement extending to middle latitudes, both north and south.

3.2. Magnetic Maps of Mean JPL-TEC: Active Versus Quiet

[20] To examine how these TEC variations might affect conditions in locales such as the daytime cusp, the JPL-TEC data are remapped to geomagnetic coordinates (magnetic latitude and local time) using the Magnetic Apex Coordinates (APEX) system [*Richmond*, 1995] and binned in the same active and quiet bins using Dst_{LG} and UT. We then are able to focus on some of the regions of interest, the cusp, and middle-latitude morning and afternoon sectors. In Figure 4 we compare morning and afternoon TEC enhancements with values in the cusp; we can quantify the relationship between middle and high latitudes, separately for the Northern and Southern Hemispheres, and look at the UT dependence of storm time cusp TEC enhancement.

[21] Examples of quiet and active average TEC maps at 1700 UT are shown in magnetic coordinates in Figures 4a and 4b, respectively. To quantify storm effects on TEC, the active/quiet TEC ratio for the 2 h period centered at 1700 UT is determined and shown in Figure 4c. The enhancement of plasma densities in the afternoon sector that is evident during magnetic storm events (e.g., Figure 1) is also evident here, extending into the auroral zone near noon and then more broadly around high latitudes on the nightside. As noted earlier, storm-driven increases in the ratio of N_2 to O in the thermosphere are the likely cause for reduction of TEC in the morning sector and much of the auroral zone [cf. *Strickland et al.*, 2001; *Immel et al.*, 2006].

[22] Mean active/quiet ratios from representative regions of the morning, cusp, and afternoon are determined from these magnetically mapped TEC ratios for each UT bin and shown in the bottom row of Figure 4. The representative regions are visually described for the Northern Hemisphere in Figure 4c. The coordinates of the regions are determined in terms of magnetic local time and latitude (reported in the figure caption). Graphs show the respective hemispheric ratio values from the morning, cusp, and afternoon regions in Figures 4d, 4e, and 4f, respectively. There are several interesting features to note. First, while the morning sector shows no significant UT-related trend in either hemisphere (Figure 4d), the Southern Hemisphere shows generally lower ratios than those in the Northern Hemisphere. This is possibly due to the larger offset of the auroral oval from the geographic pole, which would introduce greater storm heating effects and related composition disturbances at middle latitudes (in both geographic and geomagnetic coordinates). As noted earlier, geographic maps of active-quiet TEC differences show that this may be the case (see Figure 2). However, numerical simulations of the auroral-atmospheric interaction should be called upon to evaluate cause of this interhemispheric effect. Overall, the morning sector shows a very different behavior than the cusp or afternoon sector, as we now describe.

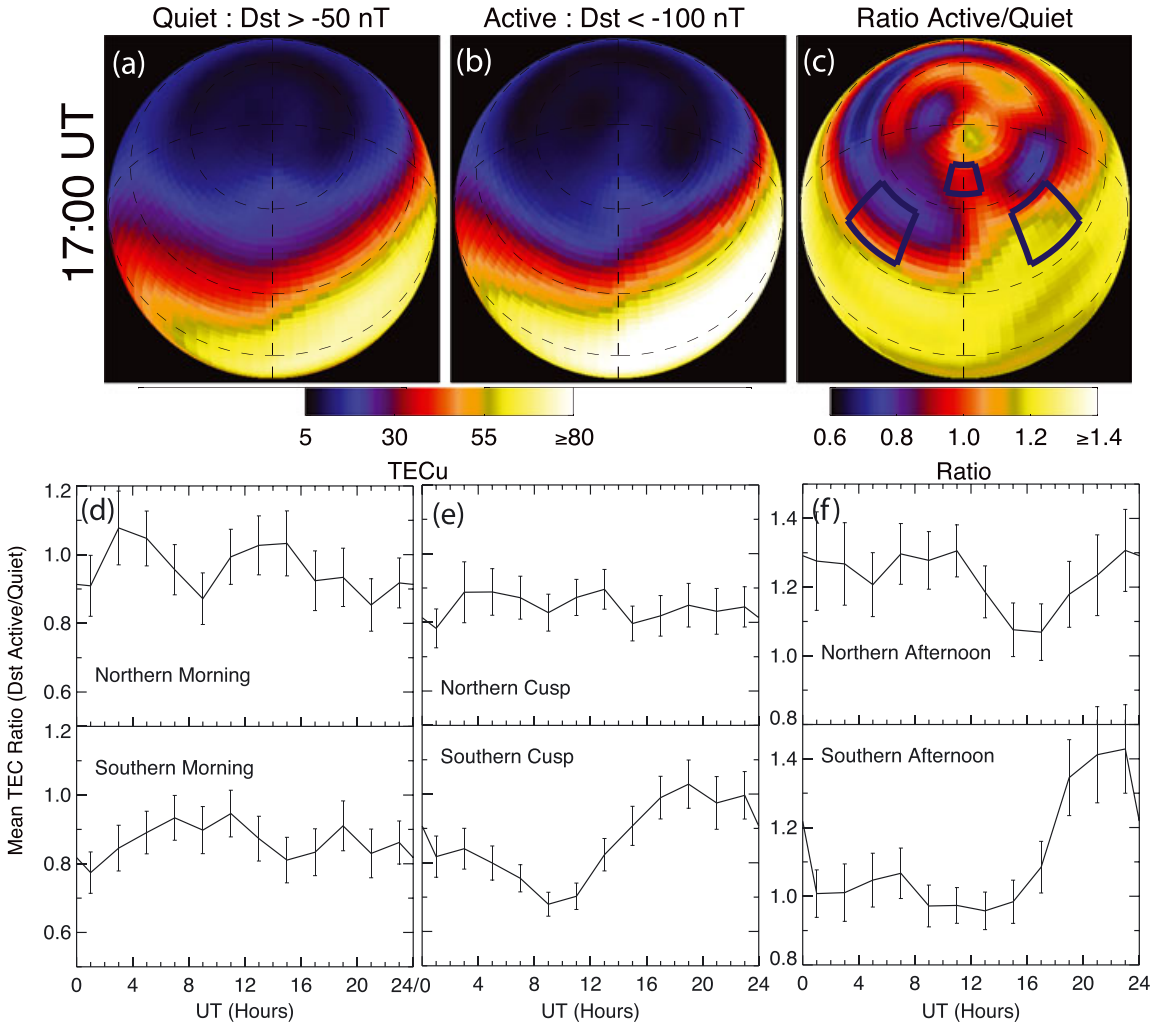

Figure 4. Global projections of mean JPL-TEC in magnetic coordinates comparing active ($Dst < -100$ nT) and quiet ($Dst > -25$ nT) periods during 1999–2005. The view is centered at noon MLT, –60° latitude, with the morning sector to the left. (a) Quiet-time mean TEC for 2 h centered at 1700 UT. (b) Active time mean TEC for 1700 UT. (c) Global projection of TEC active/quiet ratio at 17 UT in magnetic coordinates, indicating three regions of interest (cusp and morning and afternoon middle latitudes). (d) Mean TEC ratio in morning sector (±35–55°, 08–10 MLT). (e) Mean TEC ratio in the cusp (±65–75° latitude, 11–13 MLT) versus UT. (f) Mean TEC ratio in the afternoon at middle latitudes (±35–55°, 14–16 MLT).

[23] In the region of the cusp (Figure 4e) active/quiet TEC ratios in the north show mainly small variations. In the southern cusp, a more pronounced variation is found with values increasing from 0.7 at 9 UT to just over unity at 19 UT, a 40% relative enhancement. The trends with UT seen in the cusps are reflected to varying degree at middle latitudes (Figure 4f), with more than a 40% enhancement in middle-latitude TEC in the south late in the day. The Northern Hemisphere shows a more significant temporal variation in the afternoon than either the morning or the cusp, but it is smaller than the variation in the southern afternoon.

[24] In summary, significant variation in the storm time response of ionospheric TEC is evident in afternoon middle latitudes and in the vicinity of the auroral cusp. Perhaps unremarkably, no UT-dependent effect is seen in the morning sector. This is consistent with our knowledge of the formation of storm-enhanced density and SAPS, that "positive storm" effects are largely confined to the afternoon and evening sectors.

4. Relation of TEC Variability to Dst_{LG}

[25] Before further discussion of the large differences in storm time TEC variability versus geographic and geomagnetic location, it is of interest to examine the UT variation of the mean Dst_{LG} values that were used to identify active TEC maps. It is reasonable to suspect that, on average, more significant storm forcing could be occurring near the time of the afternoon/cusp TEC peak (18 to 24 UT) and so would be reflected in Dst_{LG}. However, "active" Dst_{LG} could also be relatively invariant versus UT or vary in a manner unrelated

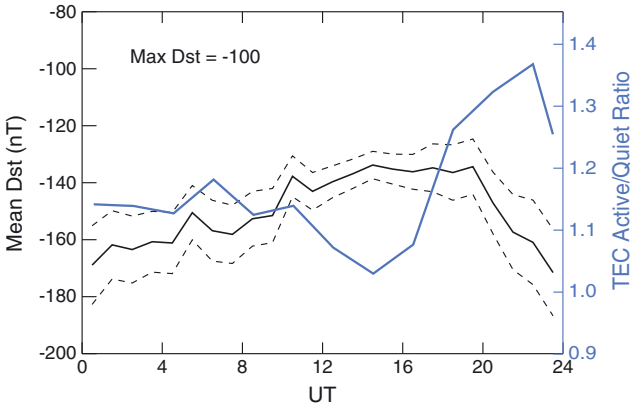

Figure 5. Mean storm Dst_{LG} (Dst_{LG} < –100 nT) for the GPS era (1998–2006) versus UT. For reference, and from the same period of time, are shown the mean of the northern and southern storm/quiet JPL-TEC ratios from afternoon middle latitudes from Figure 4e.

to the TEC values. In any case, the possible physical connection between Dst_{LG} and storm time TEC must be considered before any conclusion can be made regarding the apparently variable effectiveness of storm forcing in producing TEC enhancement.

[26] The mean storm time Dst_{LG} of the active period (1998–2005) is shown in Figure 5 (black line), with the range of one standard deviation of the mean Dst_{LG} indicated with dashed lines. Values range from –134 nT (at 14 and 19 UT) to a minimum of –172 nT at 23 UT. This is a significant variation with a single peak, much like the variation in cusp and middle-latitude TEC.

[27] For comparison, the storm/quiet TEC ratio at afternoon middle latitudes (the average of both northern and southern regions from Figure 4) is calculated and overlaid (blue line). The correspondence of this middle-latitude mean TEC ratio to the Dst_{LG} variation is striking, though the variation is nearly opposite, with a maximum TEC ratio at 22 UT versus a minimum in *Dst* at 23 UT. Directly compared, the correlation coefficient of these data sets is $r = –0.38$. Further analysis finds the largest anticorrelation of $r = –0.87$ if the TEC data are delayed by 3 h (shifted forward in time).

[28] The cusp data, where northern and southern values are combined in a manner identical to the middle-latitude ratios, demonstrate positive correlation with mean storm Dst_{LG} when directly compared ($r = 0.36$) but are strongly anticorrelated ($r = –0.83$) when the TEC data are delayed by 6 h. In both middle latitude and cusp comparisons, the largest absolute value of r is the negative value reported here. From this it is clear that beyond the comparison of the timing of the single 24 h peak in mean TEC and Dst_{LG}, periodic components in the daily variability with frequencies shorter than 24 h are more likely to be anticorrelated as well.

[29] The significant correlation between the parameters and the timing of the peak in anticorrelation informs the interpretation. Were there an indication of the peak in storm strength occurring before or at the time of greatest ionospheric enhancement, the TEC enhancement could clearly be explained as the result of stronger magnetospheric forcing. That is, the UT effect in Dst_{LG} could be indicative of greater geomagnetic storm driving with the subsequent natural effect being the creation of larger ionospheric disturbances. This hypothesis would be supported if the *Dst* minimum preceded the peak in the middle-latitude ionospheric disturbance on the known time scales of ionospheric plasma density buildup: approximately 90–180 min [cf., *Tsurutani et al.*, 2004; *Mannucci et al.*, 2005]. This analysis shows the opposite: a peak in measured magnetospheric current density following the measured peak in TEC enhancement, shifted 6 h or more from what would be expected if storm drivers associated with *Dst* were causative (based upon the 3–6 h middle and cusp latitude TEC enhancement prior to the *Dst* minimum).

[30] At this point, it is important to consider this result in the context of previous studies of geomagnetic activity as quantified by indices such as *Dst* index. The main question is whether one should reasonably expect the particular UT-dependent signature in Dst_{LG} shown in Figure 5 from any previously determined source. We investigate this in the following section.

5. UT Dependence of Dst_{LG}

[31] To evaluate how the UT-dependent, storm time ionospheric redistribution may be related to the variation in Dst_{LG}, it is important to understand the underlying trends in the Dst_{LG} index and the current understanding of their sources. Previous work using *Dst* is reviewed briefly here, and the major effects are shown to be evident in Dst_{LG}. Following that, the storm time Dst_{LG} variation (Dst_{LG} < –100 nT) in the full available range of data from 1958 to 2006 is evaluated for comparison to Dst_{LG} in the GPS era alone. The point of this latter analysis is to determine

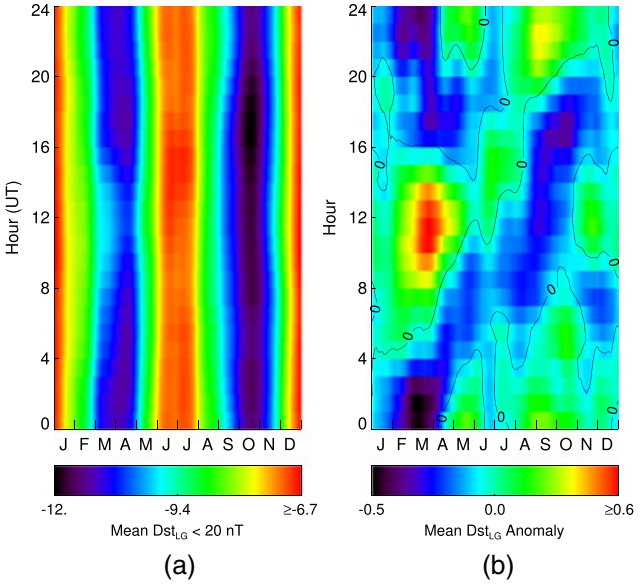

Figure 6. (a) Mean Dst_{LG} for all Dst_{LG} between 1958 and 2008, shown versus Month and UT, using a 30 day sliding averaging window. (b) Residual UT dependence after removal of daily mean Dst_{LG}. Values of Dst_{LG} greater than 20 nT (extremely quiet conditions) are excluded.

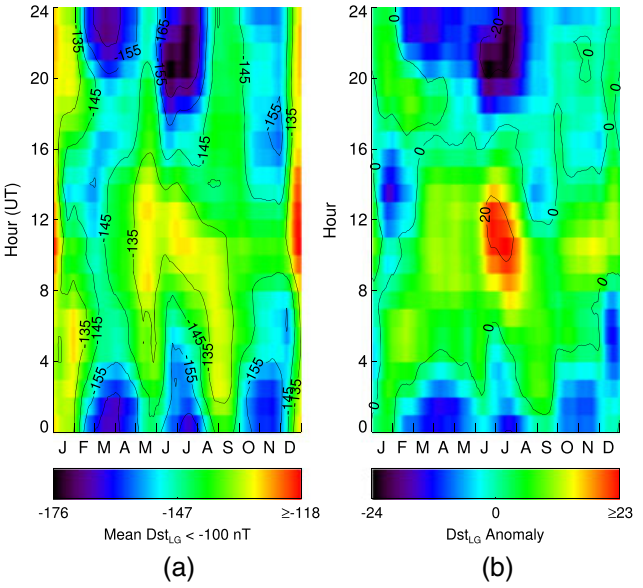

Figure 7. (a) Mean $Dst_{LG} < -100$ nT for all Dst_{LG} between 1958 and 2008, shown versus month and UT, using a 30 day sliding averaging window. (b) Residual UT dependence after removal of daily mean Dst_{LG}.

whether the UT-dependence seen in the GPS era is observed in the broader set of data available back to the International Geophysical Year.

[32] Early studies revealed one of the main underlying trends of geomagnetic activity: a semiannual variation in externally driven disturbance [*Chapman and Bartels*, 1940]. This is exhibited by more "disturbed days" and negative average *Dst* values around equinoxes. This annual variability is evident in averages of both *Dst* and Dst_{LG}. To show this effect, the mean value of hourly Dst_{LG} is determined for the 1958–2006 epoch and shown in Figure 6a. There is a clear periodic signature organized by month of the year that represents a strong semiannual variation in mean Dst_{LG}. This is the previously noted effect evident in the regular *Dst* index. The semiannual behavior was explained by *Russell and McPherron* [1973] as a consequence of seasonal changes in the alignment of Earth's magnetic field with the field embedded in the solar wind, which when favorably aligned promotes the transfer of matter and energy from the solar wind into the magnetosphere.

[33] This solar wind/magnetosphere interaction has a UT dependence as well, with a mean *Dst* minimum at 22 UT in March and 10 UT in September [*O'Brien and McPherron*, 2002]. And, though different explanations for this UT and semiannual variation in *Dst* have been proposed [cf. *Cliver et al.*, 2000], these effects are indisputably present in the *Dst* magnetic index. This UT variation varies through the year in a way made evident in this analysis of Dst_{LG} by subtracting the daily mean from each the values in Figure 6a, with the result shown in Figure 6b. Here the notable result is a clear, periodic UT variation with $n = 1$, whose peak shifts approximately 12 h between March and September. This is a clear indication of the varying interaction between Earth's magnetic field and the dominant orientation embedded in the solar wind.

[34] When the study of *Dst* is limited to disturbed values (< -100 nT), a different picture emerges. To show this in both UT and monthly simultaneously, the mean Dst_{LG} from 1958 to 2006 is determined as above but excluding $Dst_{LG} > -100$ nT. Those mean values are shown in Figure 7a. Note that, different from the above case, large changes in mean Dst_{LG} with UT are evident in the raw averages through much of the year, with a maximum (*least* negative values) around 8–10 UT for much of the year. Further interpretation of the UT variation benefits from the subtraction of the mean of the values in the 30 day sliding window, the result shown in Figure 7b. In the resulting values, it is clear that the minimum in Dst_{LG} occurs around 0 UT during most of the year, with a departure from this trend around January and February. This differs from the Russell-McPherron-type (RM-type) variation (i.e., the 12 h shift in the UT dependence between equinoxes), evident in Figure 6b. Further, the amplitude of the UT variation is on the order of 10 nT on any given day, growing to as large as 50 nT in June and July. Such a large UT variation is much greater than the magnitude of the RM-type UT variation and even the larger RM-type semiannual variation.

[35] The remarkable result is that the UT variation in storm time Dst_{LG} is present all year and is larger than any variation that can be ascribed to known variation in the solar wind to magnetosphere interaction. The UT variation accentuated around the June solstice when the UT dependence of the full set of *Dst* values (and Dst_{LG}) is at a minimum (Figure 6b). We therefore find it unlikely that the UT variation found in storm time Dst_{LG} is a result of any heretofore considered drivers of seasonal and UT variations in solar wind-magnetosphere interactions.

[36] Proceeding to examine whether the storm time Dst_{LG} shown in Figure 5 for the GPS era is representative of the similarly determined values for the entire data set going back to 1958, we calculate those values and show them in Figure 8 (green line). The GPS-era Dst_{LG} data show a larger variation but one that is consistent with the long-term trend. The long-term trend falls almost entirely within the standard deviation of the mean Dst_{LG} of the GPS-era values. We therefore find that the storm time Dst_{LG} UT-variation during

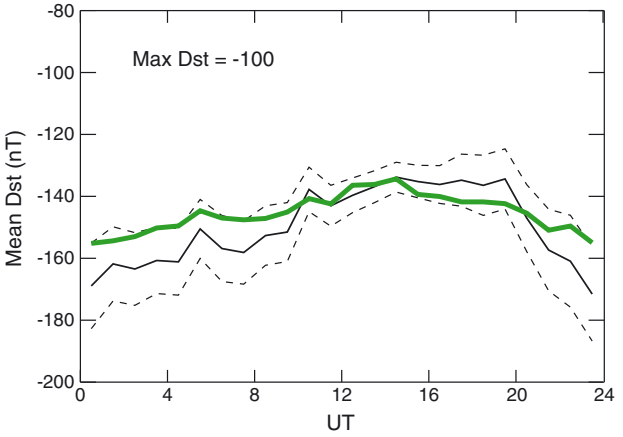

Figure 8. Mean storm Dst_{LG} ($Dst_{LG} < -100$ nT) for the modern era (1958–2008) versus UT (dark green line). Shown for reference are the same *Dst* values and uncertainties for the GPS era from Figure 5.

the 1998–2005 GPS era is likely a result of the same processes that have produced the similar effect in *Dst* going back to 1958.

[37] There is no previously reported description of this large UT-dependence of storm strength. This finding has originated naturally from an analysis where global TEC data are organized using a *Dst* cutoff limit, with no regard to storm phase. The remarkable result is that even without a more sophisticated analysis that would, for example, endeavor to organize the *Dst* and TEC data by storm phase [cf. *Katus et al.*, 2013; *Titheridge and Buonsanto*, 1988, the latter using Ap], the TEC data exhibit a variation that is well correlated with the mean storm time Dst_{LG} index. The correlation between the two parameters implies, on average, a relation between storm time ionospheric density and inner magnetospheric pressure, with the magnetosphere following the ionosphere by 3–6 h. This result must be interpreted in the light of recent research efforts, described in section 1, that have already reported that the introduction of enhanced plasma densities in the cusp should lead naturally to greater O^+ outflow rates. The UT dependence in storm time plasma densities in the region of the auroral cusp, known now from this work, may be connected naturally to conditions in the inner magnetosphere as represented by *Dst* indices.

6. Discussion

[38] The analysis presented in this paper finds that during geomagnetic storms, the global mean of afternoon middle-latitude ionospheric TEC exceeds prestorm levels, with the greatest changes occurring between 18 and 24 UT, reflecting a longitudinally prominent SED effect. Similar TEC variation is found in the region of the auroral cusp. In each region, the effect is found here to be larger in the Southern Hemisphere. An earlier study of the storm effect by *Coster et al.* [2007] found a significant effect in the Northern Hemisphere. This study does find a ∼30% enhancement in TEC at northern middle latitudes occurring in the same sector as observed by Coster et al. but with lower amplitude (Coster et al. show a change of 35 to 55 TECU, or 60%). It is important to note that the Coster et al. study focused mainly on case studies, as have others which find remarkable effects in the North American sector [e.g., *Immel et al.*, 2005]. This study finds that when all storms of a solar cycle are treated together, the "Coster effect" is twice as large in the Southern Hemisphere than in the Northern Hemisphere.

6.1. TEC Results

[39] In light of these remarkable storm time TEC results, it is important to consider the spatial distribution of data used to produce the JPL-TEC maps. These maps are model driven in the southern regions to a greater degree than the north, with larger gaps in ground station coverage of both middle latitudes and the cusp. These gaps are predictable, however, and the ground-based sampling frequency of TEC in the southern cusp has two peaks around 5 and 17 UT, so the significant difference in active/quiet ratios between those times (Figure 4e) is data driven. Southern-afternoon middle-latitude sampling also has two main peaks, at approximately 4 and 20 UT, so the large difference in active/quiet ratio between those times (cf. Figures 4f and 5) is also data driven.

[40] TEC variation in the vicinity of the southern magnetic cusp demonstrates an effect consistent with middle-latitude contribution to high-latitude TEC, though the TEC maximum in the cusp is broader in UT. Our selection of fixed location of the cusp, independent of known dependence on IMF and activity level [*Frey et al.*, 2003], may account for the less prominent variation. Another important variable comes from the generally poor chemical environment that the storm time polar thermosphere presents for maintaining high ionospheric plasma densities. For these reasons, a prominent peak at middle latitudes may not lead directly to such a prominent variation near the cusp, even if the SAPS transport is efficient.

[41] For the reasons detailed in section 4, we do not attribute the outstanding ionospheric effects observed in the South American sector to the seasonal and UT variations observed in storm time Dst_{LG}. The question remains, therefore, how this TEC enhancement comes about. The answers may lie in the fact that the magnetic field in this region is the lowest on Earth and may suffer enhanced ionospheric plasma drifts of magnitude $|\mathbf{E}|/|\mathbf{B}|$. In the simplest picture, the expansion of magnetospheric fields and SAPS should have more significant effects on the poleward and upward drift of plasma near the South American sector. This is borne out by the geographic TEC active-quiet percent differences (Figure 3a). This may combine with the 20° change in magnetic declination across the South American sector to produce plasma drifts that are unique to this geographic sector, as noted in the earlier work by *Titheridge and Buonsanto* [1988]. How this develops into a like effect for the Northern Hemisphere and across the Eastern Pacific (see Figure 3a) that lasts well after sunset is a question that remains to be resolved.

6.2. Dst_{LG} Versus TEC

[42] The examination of Dst_{LG} is performed to understand whether the above noted TEC results are possibly influenced by a UT-dependent storm forcing. We find that indeed, the Dst_{LG} values used to tag TEC maps as "active" show a UT variation. Furthermore, there is a significant correspondence between TEC and Dst_{LG}, but the maximum in TEC values *leads* the Dst_{LG} minimum (maximum in storm ring current) by 3–6 h. This provides a clear indication that the UT-dependent peak in TEC is not directly linked to changes in magnetospheric forcing, insofar as the *Dst* index provides a proxy for that forcing. Furthermore, the good anticorrelation between Dst_{LG} and time-delayed storm time TEC ($r < -0.7$ to -0.8) provides an indication that a different relation may exist. It is interesting to consider the possibility that the Dst_{LG} variation is related to the TEC enhancement itself, an enhancement that apparently develops independently of the magnetospheric forcing indicated by Dst_{LG} (and discussed in section 6.1). This bears further investigation, and we suggest a path for such an investigation in the conclusion of this report.

[43] Studies of magnetic storms, whether in hourly magnetic indices or global-scale ionospheric data, suffer for the fact that storm conditions are rare, constituting just 1–2% of all observations of geospace, and each storm is caused by a different set of initial drivers in the solar wind. Furthermore, the storm time mean Dst_{LG} determined only from values below a representative level of storm

magnitude, here –100 nT, are derived from a nonnormal distribution of extreme values. Furthermore, this study is limited to only a short period of time where GPS TEC data could be determined. Although we show that the long-term trend in Dst_{LG} is present during this period (Figure 8), we have to expect possible bias of significant large storms from this short period of study, which essentially constitutes a portion of a single solar cycle. That said, the mean Dst_{LG} sampling is very good in the 1958–2006 record, with no less than 60 samples in any one of the 30 day mean values shown in Figure 7b. Thus, the UT dependence of storm time *Dst* is quite clear in the recorded data since 1958. Follow-on work is required to improve the understanding of the events on shorter time scales and to determine improved uncertainty estimates that reflect the bimodal distribution of *Dst* values about the mean values reported here.

7. Conclusion

[44] Using continuous, global maps of ionospheric TEC over a 7+ year period, a large-scale longitudinal dependence is found in geomagnetic storm effects in the ionosphere. Geomagnetic storm forcing causes greater enhancement of TEC in the American sector than any other region of the planet, an effect first seen after noon local time and persisting into evening hours. This corresponds to a UT effect in magnetic local time maps, with large and related enhancements in the afternoon and magnetic cusp sectors after 18 UT. The Southern Hemisphere middle latitudes and cusp show the greatest UT effect, with a moderate effect at northern middle latitudes. The morning sector shows no significant UT dependence in either hemisphere.

[45] Remarkably, the Dst_{LG} values used to identify the periods of geomagnetic storms show a similar variation to the TEC at middle latitudes, delayed from that seen in the TEC values by 3–6 h. The interpretation that the UT-dependent TEC enhancements are due to a separately driven UT-dependence in Dst_{LG} is deemed unlikely for the fact that it requires an unrealistic delay of 21–18 h between Dst_{LG} storm values being reached and the resultant TEC enhancement. However, the UT dependence in Dst_{LG} bears a significant similarity to the TEC variation, which is (anti-) correlated with the TEC variation when the TEC are shifted forward in time 3 to 6 h. This supports an interpretation of a possible causal relationship, with the TEC enhancement increasing the abundance of plasma available to the polar ion fountain during storms, thus enhancing inner magnetospheric pressures and the *Dst* index. Variation in the Dst_{LG} index believed to originate in variation in the interaction between the solar wind and magnetosphere does not have the characteristics of the variation seen in the active Dst_{LG} index.

[46] JPL-TEC maps are only available for one full solar maximum, and so with a relative dearth of data (compared to *Dst*), it is necessary to determine mean TEC without consideration of all storm phases and seasonal variations. Even so, a remarkable enhancement in mean TEC is found, as large as 30–50% in the Southern Hemisphere. As the available data from global navigation satellite systems (GNNS) networks increase, it will be possible to further elucidate specific storm effects. This will be important, for at the writing of this report, the number of hours during which *Dst* values are found < –100 nT has grown little since 2006. More TEC measurements may allow for determination of storm effects at lower *Dst* thresholds (–100 nT for this report).

[47] To resolve the issues with the relatively short time period used for this report, a follow-on study that implements numerical models to capture elements of the I-T coupling and magnetospheric inputs occurring during storms that affect TEC is necessary. The goals of that study are focused first in a manner that elicits better understanding of the TEC enhancements and whether the behavior can be ascribed to the low |**B**| and large change in magnetic declination of the South American sector. The effort should concentrate on (1) the degree to which the numerical models reproduce the measured results, (2) the mechanisms that underlie the longitudinal variation in the storm enhancement, and (3) the degree to which the middle-latitude enhancements are connected to high-latitude enhancements. The Global Ionosphere-Thermosphere Model (GITM) [*Ridley et al.*, 2006] is currently being used to investigate these questions, using convection patterns that reflect storm time middle-latitude disturbances [*Ridley and Liemohn*, 2002].

[48] **Acknowledgments.** T.J.I. would like to acknowledge the support of NSF grants AGS-1103333 and AST-1019065 for this research. T.J.I. would also like to thank Tami Kovalek and Dieter Blitza at GSFC who provided ample assistance with accessing the TEC Common Data Format files using IDL. Research conducted at the Jet Propulsion Laboratory was performed under contract to the National Aeronautics and Space Administration.

[49] Robert Lysak thanks Alan Burns and Ioannis Daglis for their assistance in evaluating this paper.

References

Akasofu, S.-I. (1981), Relationships between the AE and *Dst* indices during geomagnetic storms, *J. Geophys. Res.*, *86*, 4820–4822.

Anderson, D. N. (1976), Modeling the midlatitude *F*-region ionospheric storm using east-west drift and a meridional wind, *Planet. Space Sci.*, *24*, 69–77, doi:10.1016/0032-0633(76)90063-5.

Basu, S., and C. Valladares (1999), Global aspects of plasma structures, *J. Atmos. Sol.-Terr. Phys.*, *61*, 127–139, doi:10.1016/S1364-6826(98)00122-9.

Buonsanto, M. J. (1995), A case study of the ionospheric storm dusk effect, *J. Geophys. Res.*, *100*, 23,857–23,870, doi:10.1029/95JA02697.

Buonsanto, M. J. (1999), Ionospheric storms—A review, *Space Sci. Rev.*, *88*, 563–601, doi:10.1023/A:1005107532631.

Burns, A. G., T. L. Killeen, G. R. Carignan, and R. G. Roble (1995), Large enhancements of the o/n_2 ratio in the evening sector of the winter hemisphere during geomagnetic storms, *J. Geophys. Res.*, *100*, 14,673–14,691.

Chapman, S., and J. Bartels (1940), *Geomagnetism*, chap. 11, Oxford Univ. Press, London and New York.

Clauer, R. C., and R. L. McPherron (1974), Mapping the local time–universal time development of magnetospheric substorms using mid-latitude magnetic observations, *J. Geophys. Res.*, *79*, 2811–2820.

Cliver, E. W., Y. Kamide, and A. G. Ling (2000), Mountains versus valleys: Semiannual variation of geomagnetic activity, *J. Geophys. Res.*, *105*, 2413–2424, doi:10.1029/1999JA900439.

Coster, A. J., M. J. Colerico, J. C. Foster, W. Rideout, and F. Rich (2007), Longitude sector comparisons of storm enhanced density, *Geophys. Res. Lett.*, *34*, L18105, doi:10.1029/2007GL030682.

Daglis, I. A., E. T. Sarris, and B. Wilken (1993), AMPTE/CCE CHEM observations of the ion population at geosynchronous altitudes, *Ann. Geophys.*, *11*, 685–696.

Daglis, I. A. (1997), The role of magnetosphere-ionosphere coupling in magnetic storm dynamics, in *Magnetic Storms,* vol. 98, edited by Y. K. B. T. Tsurutani, W. D. Gonzales, and J. K. Arballo, pp. 107–116, AGU, Washington, D. C.

Fok, M.-C., J. U. Kozyra, A. F. Nagy, C. E. Rasmussen, and G. V. Khazanov (1993), Decay of equatorial ring current ions and associated aeronomical consequences, *J. Geophys. Res.*, *98*, 19,381–19,393, doi:10.1029/93JA01848.

Foster, J. C. (1989), Plasma transport through the dayside cleft: A source of ionization patches in the polar cap, in *Electromagnetic Coupling*

in the Polar Clefts and Caps, edited by P. Sandholt and A. Egeland, pp. 343–354, Kluwer Acad. Pubs., Dordrecht, Netherlands.

Foster, J. C. (1993), Storm-time plasma transport at middle and high latitudes, *J. Geophys. Res.*, *98*, 1675–1689.

Foster, J. C., P. J. Erickson, A. J. Coster, J. Goldstein, and F. J. Rich (2002), Ionospheric signatures of plasmaspheric tails, *Geophys. Res. Lett.*, *29*, 1623, doi:10.1029/2002GL015067.

Foster, J. C., A. J. Coster, P. J. Erickson, W. Rideout, F. J. Rich, T. J. Immel, and B. R. Sandel (2005), Redistribution of the stormtime ionosphere and the formation of the plasmaspheric bulge, in *Inner Magnetosphere Interactions: New Perspectives from Imaging*, edited by J. Burch, M. Schulz, and H. Spence, pp. 277–289, AGU, Washington, D. C.

Frey, H. U., S. B. Mende, S. A. Fuselier, T. J. Immel, and N. Ostgaard (2003), Proton aurora in the cusp during southward IMF, *J. Geophys. Res.*, *108*, 1277, doi:10.1029/2003JA009861.

Fuller-Rowell, T. J., D. Rees, H. Rishbeth, A. G. Burns, T. L. Killeen, and R. G. Roble (1991), Modelling of composition changes during *F*-region storms—A reassessment, *J. Atmos. Terr. Phys.*, *53*, 541–550.

Fuller-Rowell, T. J., M. V. Codrescu, H. Rishbeth, R. J. Moffett, and S. Quegan (1996), On the seasonal response of the thermosphere and ionosphere to geomagnetic storms, *J. Geophys. Res.*, *101*, 2343–2353.

Goldstein, J. (2006), Plasmasphere response: Tutorial and review of recent imaging results, *Space Sci. Rev.*, *124*, 203–216, doi:10.1007/s11214-006-9105-y.

Goldstein, J., B. R. Sandel, M. R. Hairston, and P. H. Reiff (2003), Control of plasmaspheric dynamics by both convection and sub-auroral polarization stream, *Geophys. Res. Lett.*, *2243*(24), doi:10.1029/2003GL018390.

Heelis, R. A., J. J. Sojka, M. David, and R. W. Schunk (2009), Storm time density enhancements in the middle-latitude dayside ionosphere, *J. Geophys. Res.*, *114*, A03315, doi:10.1029/2008JA013690.

Hunsucker, R. D., and J. K. Hargreaves (2002), *The High-Latitude Ionosphere and Its Effects on Radio Propagation*, Cambridge Univ. Press, Cambridge, U. K.

Immel, T. J., J. D. Craven, and A. C. Nicholas (2000), The DE-1 auroral imager's response to the FUV dayglow for thermospheric studies, *J. Atmos. Solar-Terr. Phys.*, *62*, 47–64.

Immel, T. J., G. Crowley, J. D. Craven, and R. G. Roble (2001), Dayside enhancements of thermospheric O/N_2 following magnetic storm onset, *J. Geophys. Res.*, *106*, 15,471–15,488.

Immel, T. J., J. C. Foster, A. J. Coster, S. B. Mende, and H. U. Frey (2005), Global storm time plasma redistribution imaged from the ground and space, *Geophys. Res. Lett.*, *32*, L03107, doi:10.1029/2004GL021120.

Immel, T. J., G. Crowley, C. L. Hackert, J. D. Craven, and R. G. Roble (2006), Effect of IMF B_y on thermospheric composition at high and middle latitudes: 2. Data comparisons, *J. Geophys. Res.*, *111*, A10312, doi:10.1029/2005JA011372.

Jones, K. L., and H. Rishbeth (1971), The origin of storm increases of mid-latitude *F*-layer electron concentration, *J. Atmos. Terr. Phys.*, *33*, 391–401.

Katus, R. M., M. W. Liemohn, D. L. Gallagher, A. Ridley, and S. Zou (2013), Evidence for potential and inductive convection during intense geomagnetic events using normalized superposed epoch analysis, *J. Geophys. Res.*, *118*, 181–191, doi:10.1029/2012JA017915.

Kintner, P. M., B. Ledvina, E. de Paula, J. Makela, and J. Sojka (2003), The advantages of cheap, connected, and plentiful GNSS observations, *Eos Trans. AGU, 84*(46), Fall Meet. Suppl., Abstract SH52B-02.

Lanzerotti, L. J., L. L. Cogger, and M. Mendillo (1975), Latitude dependence of ionosphere total electron content—Observations during sudden commencement storms, *J. Geophys. Res.*, *80*, 1287–1306, doi:10.1029/JA080i010p01287.

Liemohn, M. W., J. U. Kozyra, V. K. Jordanova, G. V. Khazanov, M. F. Thomsen, and T. E. Cayton (1999), Analysis of early phase ring current recovery mechanisms during geomagnetic storms, *Geophys. Res. Lett.*, *26*, 2845–2848, doi:10.1029/1999GL900611.

Love, J. J., and J. L. Gannon (2009), Revised *Dst* and the epicycles of magnetic disturbance: 1958–2007, *Ann. Geophys.*, *27*, 3101–3131.

Lui, A. T. Y., P. C. Brandt, and D. G. Mitchell (2005), Observations of energetic neutral oxygen by IMAGE/HENA and Geotail/EPIC, *Geophys. Res. Lett.*, *32*, L13104, doi:10.1029/2005GL022851.

Mannucci, A. J., B. D. Wilson, D. N. Yuan, C. H. Ho, U. J. Lindqwister, and T. F. Runge (1998), A global mapping technique for GPS-derived ionospheric total electron content measurements, *Radio Sci.*, *33*, 565–582, doi:10.1029/97RS02707.

Mannucci, A. J., B. T. Tsurutani, B. A. Iijima, A. Komjathy, A. Saito, W. D. Gonzalez, F. L. Guarnieri, J. U. Kozyra, and R. Skoug (2005), Dayside global ionospheric response to the major interplanetary events of October 29–30, 2003 "Halloween Storms", *Geophys. Res. Lett.*, *32*, L12S02, doi:10.1029/2004GL021467.

Mendillo, M., M. D. Papagiannis, and J. A. Klobuchar (1970), Ionospheric storms at midlatitudes, *Radio Sci.*, *5*, 895–898, doi:10.1029/RS005i006p00895.

Mendillo, M., M. D. Papagiannis, and J. A. Klobuchar (1972), Average behavior of the midlatitude *F*-region parameters N_T, N_{max}, and τ during geomagnetic storms, *J. Geophys. Res.*, *77*, 4891–4895, doi:10.1029/JA077i025p04891.

Mursula, K., L. Holappa, and A. Karinen (2010), Uneven weighting of stations in the *Dst* index, *J. Atmos. Solar-Terr. Phys.*, *73*, 316–322, doi:10.1016/j.jastp.2010.04.007.

Nicholas, A. C., J. D. Craven, and L. A. Frank (1997), A survey of large-scale variations in thermospheric oxygen column density with magnetic activity as inferred from observations of the FUV dayglow, *J. Geophys. Res.*, *102*, 4493–4510.

O'Brien, T. P., and R. L. McPherron (2002), Seasonal and diurnal variation of *Dst* dynamics, *J. Geophys. Res.*, *107*, 1341, doi:10.1029/2002JA009435.

Prölss, G. W. (1980), Magnetic storm associated perturbations of the upper atmosphere: Recent results obtained by satellite-borne gas analyzers, *Rev. Geophys.*, *18*, 183–202.

Prölss, G. W. (2008), Ionospheric storms at mid-latitude: A short review, in *Midlatitude Lonospheric Dynamics and Disturbances* vol. 181, edited by P. M. Kintner et al., pp. 9–24, AGU, Washington, D. C., doi:10.1029/181GM03.

Prölss, G. W., and J. D. Craven (1998), Perturbations of the FUV dayglow and ionospheric storm effects, *Adv. Space Res.*, *22*(1), 129–132.

Prölss, G. W., and M. Roemer (1987), Thermospheric storms, *Adv. Space Res.*, *7*(10), 223–235.

Pryse, S., R. Sims, J. Moen, L. Kersley, D. Lorentzen, and W. Denig (2004), Evidence for solar-production as a source of polar-cap plasma, *Ann. Geophys.*, *22*, 1093–1102.

Richmond, A. D. (1995), Ionospheric electrodynamics using magnetic apex coordinates, *J. Geomagn. Geoelectr.*, *47*, 191–212.

Ridley, A. J., and M. W. Liemohn (2002), A model-derived storm time asymmetric ring current driven electric field description, *J. Geophys. Res.*, *107*(A8), 1151, doi:10.1029/2001JA000051.

Ridley, A. J., Y. Deng, and G. Tóth (2006), The global ionosphere thermosphere model, *J. Atmos. Solar-Terr. Phys.*, *68*, 839–864, doi:10.1016/j.jastp.2006.01.008.

Roble, R. G. (1977), *The Upper Atmosphere and Magnetosphere*, National Academy of Sciences, The Univ. of Michigan.

Rodger, A. S., R. J. Moffett, and S. Quegan (1992), The role of ion drift in the formation of ionisation troughs in the mid- and high-latitude ionosphere—A review, *J. Atmos. Terr. Phys.*, *54*, 1–30.

Russell, C. T., and R. L. McPherron (1973), Semiannual variation of geomagnetic activity, *J. Geophys. Res.*, *78*, 92–108.

Sharp, R. D., R. G. Johnson, and E. G. Shelley (1976), The morphology of energetic O/+/ ions during two magnetic storms—Temporal variations, *J. Geophys. Res.*, *81*, 3283–3291, doi:10.1029/JA081i019p03283.

Strangeway, R. J., C. T. Russell, C. W. Carlson, J. P. McFadden, R. E. Ergun, M. Temerin, D. M. Klumpar, W. K. Peterson, and T. E. Moore (2000), Cusp field-aligned currents and ion outflows, *J. Geophys. Res.*, *105*, 21,129–21,142, doi:10.1029/2000JA900032.

Strickland, D. J., R. E. Daniell, and J. D. Craven (2001), Negative ionospheric storm coincident with DE 1-observed thermospheric disturbance on October 14, 1981, *J. Geophys. Res.*, *106*, 21,049–21,062.

Sugiura, M. (1964), *Hourly Values of Equatorial Dst for the IGY*, chap. 9, vol. 35, Annual International Geophysical Year, Pergamon press, New York.

Titheridge, J. E., and M. J. Buonsanto (1988), A comparison of Northern and Southern Hemisphere TEC storm behaviour, *J. Atmos. Terr. Phys.*, *50*, 763–780.

Tsurutani, B., et al. (2004), Global dayside ionospheric uplift and enhancement associated with interplanetary electric fields, *J. Geophys. Res.*, *109*, A08302, doi:10.1029/2003JA010342.

Zeng, W., and J. L. Horwitz (2008), Storm enhanced densities (SED) as possible sources for Cleft Ion Fountain dayside ionospheric outflows, *J. Geophys. Res.*, *35*, L04103, doi:10.1029/2007GL032511.

Zhang, J., et al. (2007), Understanding storm-time ring current sources through data-model comparisons of a moderate storm, *J. Geophys. Res.*, *112*, A04208, doi:10.1029/2006JA011846.

Zou, S., M. B. Moldwin, A. Coster, L. R. Lyons, and M. J. Nicolls (2011), GPS TEC observations of dynamics of the mid-latitude trough during substorms, *Geophys. Res. Lett.*, *38*, L14109, doi:10.1029/2011GL048178.